

Supplemental information for

**Thermal decomposition of peroxyacrylic nitric anhydride (APAN)**

5 Amanda L. Gomez, Kevin D. Easterbrook, Nicole M. Johnson, Shana Johnson, and Hans D. Osthoff  
Department of Chemistry, University of Calgary, 2500 University Drive N.W., Calgary, Alberta, Canada  
T2N 1N4

*Correspondence to* Hans D. Osthoff ([hosthoff@ucalgary.ca](mailto:hosthoff@ucalgary.ca))

10

**Contents**

Table S1. Experiment schedule for experiments with APAN.....	2
15 Table S1 (continued).....	3
Table S2. Experiment schedule for experiments with PAN. ....	4
Figure S1. Sample chromatograms of PANs. ....	5
Figure S2. Plot of $\ln(C/C_0)$ for PAN vs. $t_{\text{res}}$ at a temperature of 313.2 K.....	6
Figure S3. Near-surface smoke forecast for May 16, 2023. ....	7
20 Figure S4. Scatter plots of PPN and APAN vs. PAN during FOOBAR.....	8
Figure S5. Plots of $\ln(C_0/C_t)$ for PAN, PPN and APAN vs. time for selected periods observed during FOOBAR. ....	9
References.....	10

25

**Table S1.** Experiment schedule for experiments with APAN. The zero air (ZA) and nitric oxide (NO) flow rates are expressed in set point voltage of the 100 sccm capacity mass flow controllers, where 5.00 V equals full scale. All stated uncertainties are at the  $\pm 1\sigma$  level. Loss rate constants of APAN ( $k_{-2}$ , far right column) were calculated by dividing  $-\ln \left( \frac{C_t}{C_0} \right)$  by  $t_{\text{res}}$  and assuming random and independent error propagation.

Internal reference	T (°C)	P (Torr)	ZA Flow (V)	NO Flow (V)	$t_{\text{res}}$ (s)	$\ln \left( \frac{C_t}{C_0} \right)$	$k_{-2}$ (s <sup>-1</sup> )
NJ 230320-1	47.50±0.01	659.6±0.1	4.00±0.01	0.75±0.01	109.3±1.0	-1.47±0.19	(1.34±0.18)×10 <sup>-2</sup>
NJ 230320-2	47.50±0.01	660.1±0.1	5.00±0.01	0.75±0.01	90.3±0.8	-1.20±0.16	(1.33±0.18)×10 <sup>-2</sup>
NJ 230324-1	47.50±0.01	661.1±0.1	3.50±0.01	0.75±0.01	122.4±1.1	-1.59±0.08	(1.30±0.07)×10 <sup>-2</sup>
NJ 230324-2	47.50±0.01	661.0±0.1	4.50±0.01	0.75±0.01	99.1±0.9	-1.33±0.15	(1.35±0.15)×10 <sup>-2</sup>
NJ 230327-1	47.50±0.01	670.1±0.1	3.75±0.01	0.75±0.01	117.2±1.1	-1.56±0.11	(1.33±0.09)×10 <sup>-2</sup>
NJ 230327-2	47.50±0.01	671.3±0.1	4.25±0.01	0.75±0.01	105.6±1.0	-1.44±0.11	(1.36±0.11)×10 <sup>-2</sup>
NJ 230227-1	45.00±0.01	653.4±0.1	2.50±0.01	0.75±0.01	159.4±1.5	-1.54±0.06	(9.6±0.4)×10 <sup>-3</sup>
NJ 230227-2	45.00±0.01	652.5±0.1	3.50±0.01	0.75±0.01	121.7±1.1	-1.12±0.03	(9.2±0.2)×10 <sup>-3</sup>
NJ 230303-1	45.00±0.01	653.5±0.1	1.50±0.01	0.75±0.01	230.3±2.4	-2.18±0.11	(9.5±0.5)×10 <sup>-3</sup>
NJ 230303-2	45.00±0.01	653.7±0.1	3.00±0.01	0.75±0.01	138.2±1.3	-1.28±0.10	(9.2±0.8)×10 <sup>-3</sup>
NJ 230303-3	45.00±0.01	653.6±0.1	5.00±0.01	0.75±0.01	90.1±0.8	-0.89±0.07	(9.8±0.8)×10 <sup>-3</sup>
NJ 230306-1	45.00±0.01	667.5±0.1	4.00±0.01	0.75±0.01	111.4±1.0	-1.19±0.10	(10.6±0.9)×10 <sup>-3</sup>
AG 230425-1	42.00±0.01	663.1±0.1	3.00±0.01	0.75±0.01	141.6±1.3	-0.98±0.04	(6.9±0.3)×10 <sup>-3</sup>
AG 230425-2	42.00±0.01	663.1±0.1	1.50±0.01	0.75±0.01	235.9±2.5	-1.66±0.14	(7.1±0.6)×10 <sup>-3</sup>
AG 230425-4	42.00±0.01	663.1±0.1	2.50±0.01	0.75±0.01	163.3±1.6	-1.13±0.09	(6.9±0.5)×10 <sup>-3</sup>
AG 230602-2	42.00±0.01	667.9±0.1	3.75±0.01	0.75±0.01	118.8±1.1	-0.65±0.06	(5.5±0.5)×10 <sup>-3</sup>
AG 230602-3	42.00±0.01	667.9±0.1	1.79±0.01	0.75±0.01	210.5±2.1	-1.39±0.36	(6.6±1.7)×10 <sup>-3</sup>
AG 230606-1	42.00±0.01	665.7±0.1	4.45±0.01	0.75±0.01	102.5±0.9	-0.76±0.07	(7.4±0.7)×10 <sup>-3</sup>
AG 230228-1	40.00±0.01	652.8±0.1	1.50±0.01	0.75±0.01	233.8±2.4	-1.19±0.05	(5.1±0.2)×10 <sup>-3</sup>
AG 230228-2	40.00±0.01	653.5±0.1	2.00±0.01	0.75±0.01	191.5±1.9	-0.99±0.11	(5.2±0.6)×10 <sup>-3</sup>
AG 230228-3	40.00±0.01	654.2±0.1	2.50±0.01	0.75±0.01	162.2±1.5	-0.87±0.06	(5.4±0.4)×10 <sup>-3</sup>
AG 230301-1	40.00±0.01	655.9±0.1	3.00±0.01	0.75±0.01	140.9±1.3	-0.81±0.05	(5.7±0.4)×10 <sup>-3</sup>
AG 230301-2	40.00±0.01	654.5±0.1	3.50±0.01	0.75±0.01	124.1±1.1	-0.63±0.04	(5.1±0.3)×10 <sup>-3</sup>
AG 230301-3	40.00±0.01	649.7±0.1	4.00±0.01	0.75±0.01	107.2±1.0	-0.51±0.04	(4.8±0.4)×10 <sup>-3</sup>
AG 230612-3	40.00±0.01	665.5±0.1	4.25±0.01	0.75±0.01	110.2±1.0	-0.68±0.12	(6.2±1.1)×10 <sup>-3</sup>

30 **Table S1 (continued).**

<b>Internal reference</b>	<b>T</b> (°C)	<b>P</b> (Torr)	<b>ZA Flow</b> (V)	<b>NO Flow</b> (V)	<b>t<sub>res</sub></b> (s)	<b>ln</b> <left(< left=""><b>C<sub>t</sub></b><right>/<b>C<sub>0</sub></b><right)< th=""><th><b>k<sub>.2</sub></b> (s<sup>-1</sup>)</th></right)<></right></left(<>	<b>k<sub>.2</sub></b> (s <sup>-1</sup> )
NJ 230403-2	37.50±0.01	661.0±0.1	3.00±0.01	0.75±0.01	143.2±1.3	-0.40±0.02	(2.8±0.2)×10 <sup>-3</sup>
NJ 230403-3	37.50±0.01	661.1±0.1	4.00±0.01	0.75±0.01	113.0±1.0	-0.44±0.06	(3.9±0.5)×10 <sup>-3</sup>
AG 230713-1	37.50±0.01	665.4±0.1	2.75±0.01	0.75±0.01	154.4±1.5	-0.56±0.02	(3.6±0.2)×10 <sup>-3</sup>
AG 230713-2	37.50±0.01	665.4±0.1	1.50±0.01	0.75±0.01	240.2±2.5	-0.90±0.06	(3.8±0.2)×10 <sup>-3</sup>
KE 230714-1	37.50±0.01	668.0±0.1	4.00±0.01	0.75±0.01	114.2±1.0	-0.49±0.05	(4.3±0.5)×10 <sup>-3</sup>
KE 230717-1	37.50±0.01	660.7±0.1	3.00±0.01	0.75±0.01	143.1±1.3	-0.62±0.09	(4.3±0.6)×10 <sup>-3</sup>
KE 230717-2	37.50±0.01	658.9±0.1	3.50±0.01	0.75±0.01	125.9±1.2	-0.45±0.03	(3.6±0.3)×10 <sup>-3</sup>
KE 230719-1	37.50±0.01	670.9±0.1	1.75±0.01	0.75±0.01	217.9±2.2	-0.61±0.03	(2.8±0.1)×10 <sup>-3</sup>
AG 230426-1	35.50±0.01	661.5±0.1	2.00±0.01	0.75±0.01	196.6±2.0	-0.46±0.08	(2.4±0.4)×10 <sup>-3</sup>
AG 230426-2	35.50±0.01	661.5±0.1	4.25±0.01	0.75±0.01	108.1±1.0	-0.28±0.03	(2.6±0.3)×10 <sup>-3</sup>
AG 230426-3	35.50±0.01	661.5±0.1	3.00±0.01	0.75±0.01	144.2±1.3	-0.30±0.09	(2.1±0.6)×10 <sup>-3</sup>
AG 230427-1	35.50±0.01	667.8±0.1	1.75±0.01	0.75±0.01	218.4±2.2	-0.56±0.08	(2.5±0.4)×10 <sup>-3</sup>
AG 230609-1	35.50±0.01	667.0±0.1	3.50±0.01	0.75±0.01	128.3±1.2	-0.36±0.03	(2.8±0.3)×10 <sup>-3</sup>
KE 230719-2	35.50±0.01	669.5±0.1	2.50±0.01	0.75±0.01	168.4±1.6	-0.38±0.02	(2.2±0.1)×10 <sup>-3</sup>
KE 230721-1	35.50±0.01	667.1±0.1	2.25±0.01	0.75±0.01	181.8±1.8	-0.29±0.10	(1.6±0.6)×10 <sup>-3</sup>
KE 230721-2	35.50±0.01	665.4±0.1	4.75±0.01	0.75±0.01	98.9±0.9	-0.21±0.03	(2.2±0.3)×10 <sup>-3</sup>
AG 230428-1	30.00±0.01	667.8±0.1	2.00±0.01	0.75±0.01	202.1±2.0	-0.32±0.04	(1.6±0.2)×10 <sup>-3</sup>
AG 230428-2	30.00±0.01	667.8±0.1	3.25±0.01	0.75±0.01	138.9±1.3	-0.24±0.05	(1.7±0.4)×10 <sup>-3</sup>
KE 230711-1	30.00±0.01	663.3±0.1	1.50±0.01	0.75±0.01	245.4±1.0	-0.23±0.02	(1.0±0.1)×10 <sup>-3</sup>
KE 230711-2	30.00±0.01	663.3±0.1	5.00±0.01	0.75±0.01	96.0±2.6	-0.12±0.04	(1.3±0.4)×10 <sup>-3</sup>
AG 230712-2	30.00±0.01	667.8±0.1	2.75±0.01	0.75±0.01	159.3±1.5	-0.21±-0.02	(1.3±0.1)×10 <sup>-3</sup>
<sup>1</sup> KE 230808-1	22.0±0.1	663.3±0.1	0.50±0.01	0.75±0.01	523±7	-0.25±0.14	(4.8±2.6)×10 <sup>-4</sup>
KE 230809-1b	22.00±0.01	659.6±0.1	0.50±0.01	0.75±0.01	451±6	-0.275±0.006	(6.1±0.2)×10 <sup>-4</sup>
KE 230809-1c	22.00±0.01	659.6±0.1	0.50±0.01	0.75±0.01	451±6	-0.293±0.008	(6.5±0.2)×10 <sup>-4</sup>
<sup>2</sup> KE 230810-1b	22.00±0.01	658.3±0.1	0.50±0.01	0.75±0.01	450±6	-0.218±0.006	(4.9±0.2)×10 <sup>-4</sup>
<sup>2</sup> KE 230810-1c	22.00±0.01	657.7±0.1	0.50±0.01	0.75±0.01	450±6	-0.254±0.014	(5.7±0.3)×10 <sup>-4</sup>
<sup>1,2</sup> KE 230810-2	22.8±0.1	658.5±0.1	0.50±0.01	0.75±0.01	518±7	-0.271±0.089	(5.2±1.7)×10 <sup>-4</sup>

<sup>1</sup> Experiment with Teflon coated reactor. <sup>2</sup>Humidified gas stream.

**Table S2.** Experiment schedule for experiments with PAN. The zero air (ZA) and nitric oxide (NO) flow rates are expressed in set point voltage of the 100 sccm capacity mass flow controllers, where 5.00 V equals full scale. All stated uncertainties are at the  $\pm 1\sigma$  level. Loss rate constants of PAN ( $k_{-2}$ , far right column)  
 35 were calculated by dividing  $-\ln\left(\frac{C_t}{C_0}\right)$  by  $t_{\text{res}}$  and assuming random and independent error propagation.

Internal reference	T (°C)	P (Torr)	ZA Flow (V)	NO Flow (V)	$t_{\text{res}}$ (s)	$\ln\left(\frac{C_t}{C_0}\right)$	$k_{-2}$ (s <sup>-1</sup> )
AG 230725-1	40.00±0.01	661.3±0.1	3.00±0.01	0.75±0.01	0.52±0.09	0.52±0.09	(3.6±0.7)×10 <sup>-3</sup>
KE 230726-1	40.00±0.01	662.0±0.1	2.25±0.01	0.75±0.01	0.57±0.08	0.57±0.08	(3.2±0.5)×10 <sup>-3</sup>
KE 230726-2	40.00±0.01	661.3±0.1	4.00±0.01	0.75±0.01	0.46±0.05	0.46±0.05	(4.1±0.4)×10 <sup>-3</sup>
AG 230728-2	40.00±0.01	671.1±0.1	1.75±0.01	0.75±0.01	0.60±0.01	0.60±0.01	(2.8±0.6)×10 <sup>-3</sup>
AG 230728-3	40.00±0.01	671.1±0.1	3.35±0.01	0.75±0.01	0.41±0.02	0.41±0.02	(3.1±0.2)×10 <sup>-3</sup>
AG 230731-1	40.00±0.01	664.9±0.1	1.55±0.01	0.75±0.01	0.80±0.05	0.80±0.05	(3.4±0.2)×10 <sup>-3</sup>
AG 230731-2	40.00±0.01	664.9±0.1	5.01±0.01	0.75±0.01	0.34±0.02	0.34±0.02	(3.7±0.2)×10 <sup>-3</sup>
KE 230802-1	40.00±0.01	667.2±0.1	1.00±0.01	0.75±0.01	1.03±0.08	1.03±0.08	(3.4±0.3)×10 <sup>-3</sup>

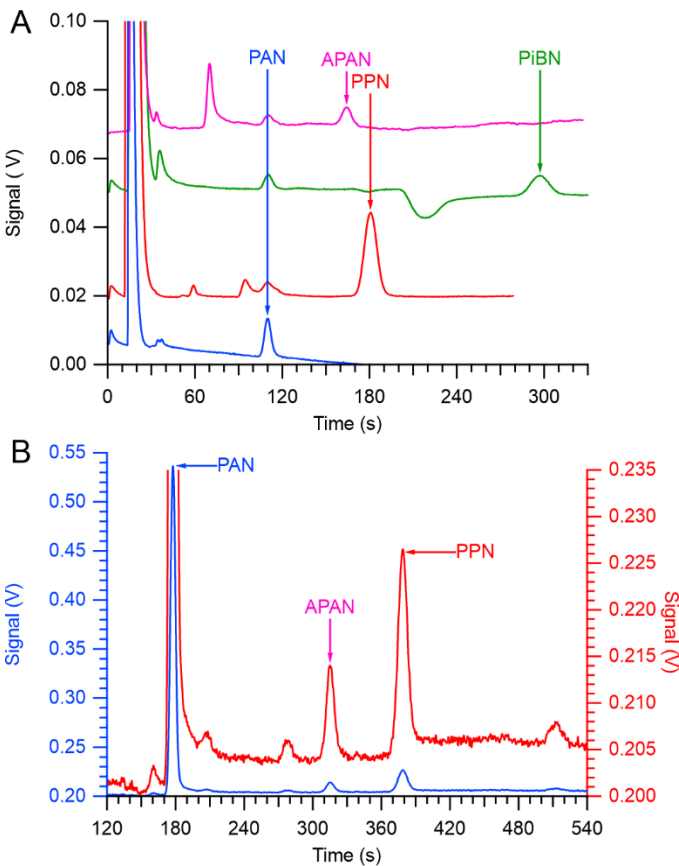
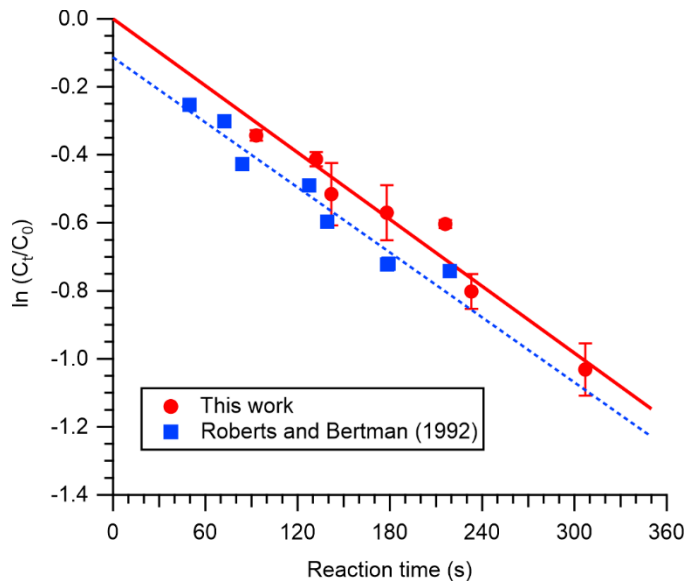


**Figure S1.** Sample chromatograms of PANs. **(A)** Laboratory data collected on an RTX-200 megabore column at a column flow rate of  $34.0 \text{ mL min}^{-1}$ , vertically offset for clarity. Samples containing PAN, 40 PPN, and PiBN were generated photochemically, whereas APAN was eluted from a diffusion source containing a synthetic sample spiked with a PAN sample. **(B)** Ambient air chromatogram collected on an RTX-1701 megabore column at a He flow rate of  $37.4 \text{ mL min}^{-1}$ , observed on May 20, 2023, 19:00 coordinated universal time (UTC) during the FOOBAR campaign. The PAN, PPN and APAN mixing ratios were 3.36 ppbv, 454 pptv, and 219 pptv, respectively.



45

**Figure S2.** Plot of  $\ln(C_t/C_0)$  for PAN vs.  $t_{\text{res}}$  at a temperature of 313.2 K. Error bars are at the  $1\sigma$  precision level. The superimposed data from Roberts and Bertman (1992) were digitized from Figure 2 of their manuscript using Engauge Digitizer software (Mitchell, 2021). Linear regression of our data yields a slope of  $k_{-2} = (3.3 \pm 0.1) \times 10^{-3} \text{ s}^{-1}$  consistent with the value reported by Roberts and Bertman of  $(2.9 \pm 0.5) \times 10^{-3} \text{ s}^{-1}$ .

50

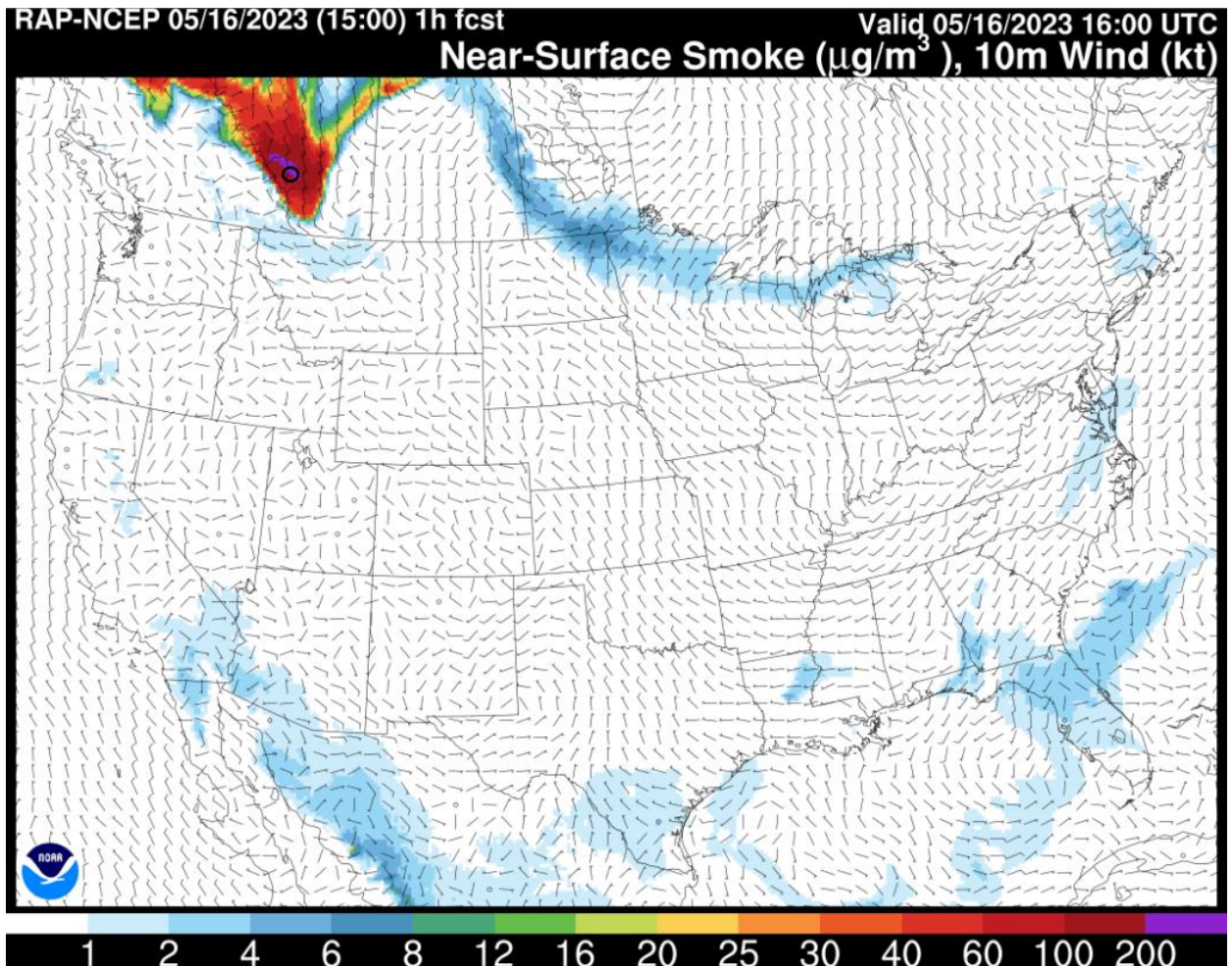


**Figure S3.** Near-surface smoke forecast for May 16, 2023. Image derived from the Rapid Refresh (RAP) archive, a continental-scale hourly assimilation/modelling system operational at the National Center for Environment Prediction (NCEP) of the National Oceanic and Atmospheric Administration (NOAA) from 55 archived simulations (<https://rapidrefresh.noaa.gov/hrrr/>). The black circle marks the approximate location of the City of Calgary.

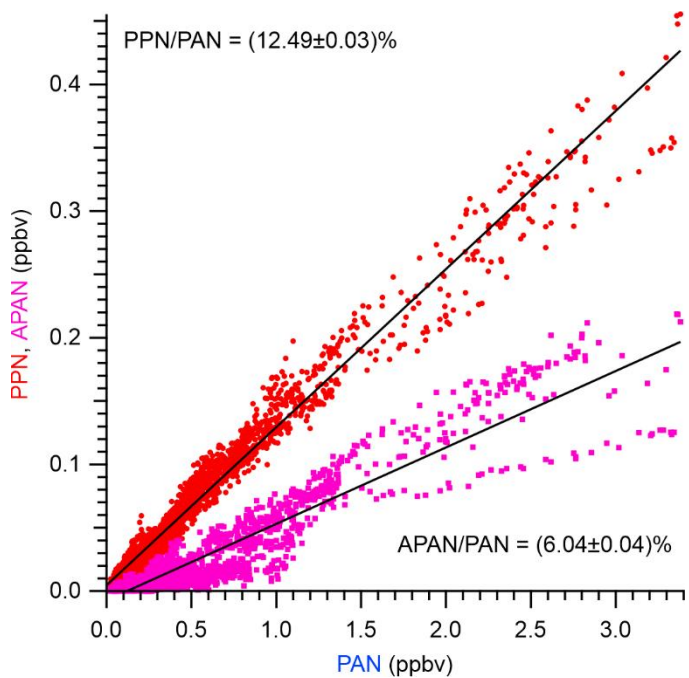


**Figure S4.** Scatter plots of PPN and APAN vs. PAN during FOOBAR.

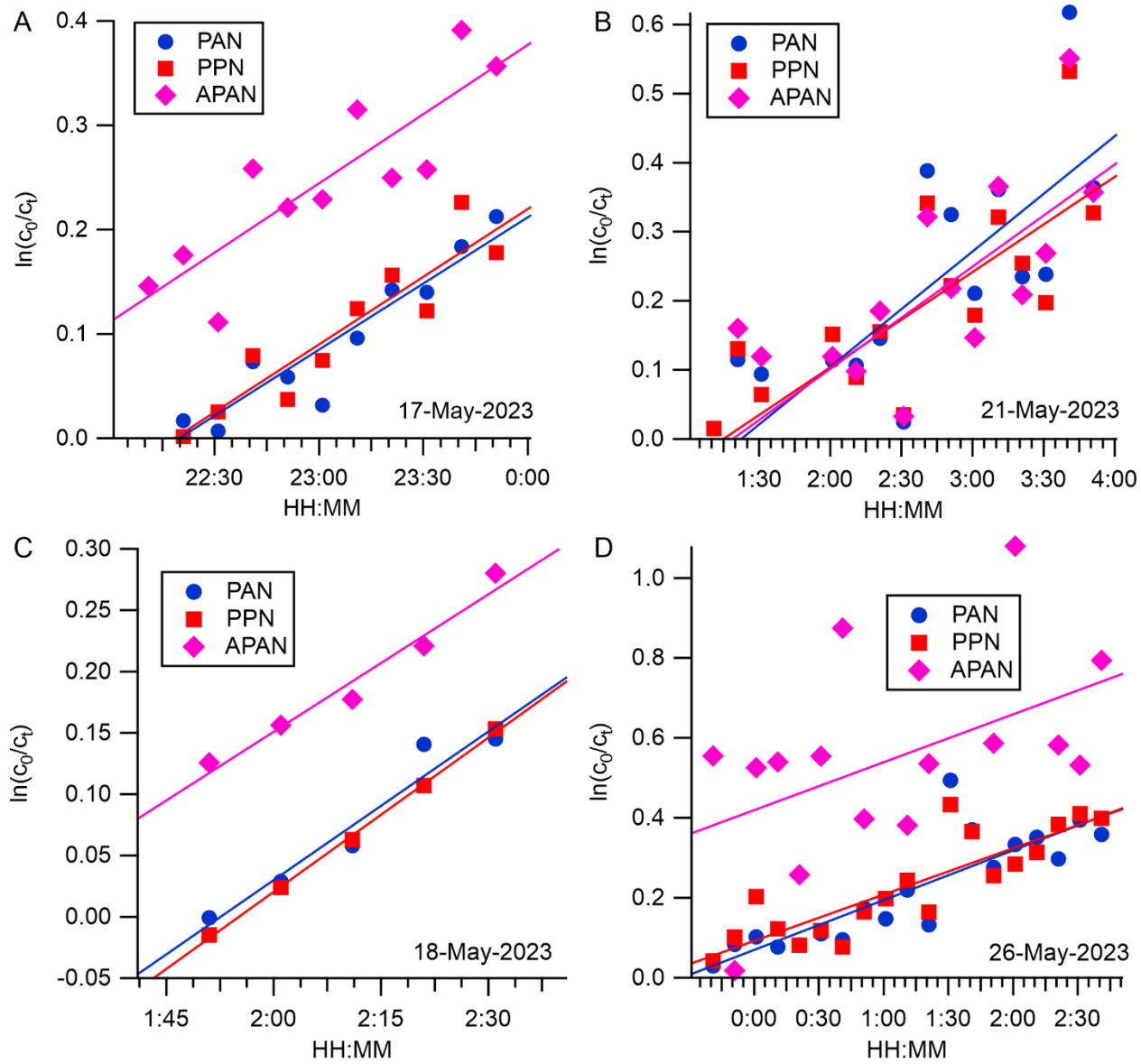


**Figure S5.** Plots of  $\ln(C_0/C_t)$  for PAN, PPN and APAN vs. time for selected periods observed during FOOBAR. The vertical offsets arise from the starting value, i.e., the respective choices of  $C_0$ .

65 **References**

- Mitchell, M.: Engauge Digitizer: doi: 10.5281/zenodo.3941227, 2021.
- Roberts, J. M., and Bertman, S. B.: The thermal decomposition of peroxyacetic nitric anhydride (PAN) and peroxymethacrylic nitric anhydride (MPAN), Internat. J. Chem. Kin., 24, 297-307,  
70 10.1002/kin.550240307, 1992.